

in terms of the scattering angle θ . Thus for unpolarized radiation,

$$|S_{\text{out}}| = \frac{e^4 E_0^2}{16\pi m_e^2 c^3 r^2} (1 + \cos^2 \theta) \quad \text{erg cm}^2 \text{ sec}^{-1} \quad (4-8)$$

The energy per unit time passing through a segment of area dA perpendicular to \mathbf{r} which is bounded by a solid angle element $d\Omega = dA/r^2$ is therefore

$$|S_{\text{out}}| dA = \frac{1}{r^2} \frac{e^4 E_0^2}{16\pi m_e^2 c^3} (1 + \cos^2 \theta) dA = \frac{e^4 E_0^2}{16\pi m_e^2 c^3} (1 + \cos^2 \theta) d\Omega \quad (4-9)$$

The differential cross section for re-emission of radiation (Thomson scattering) into a solid angle $d\Omega$ is, by definition, the ratio of this quantity to the incident intensity $|S_{\text{in}}|$,

$$\sigma_{\text{Th}}(\theta) d\Omega = \frac{|S_{\text{out}}| dA}{|S_{\text{in}}|} = \frac{1}{2} \left(\frac{e^2}{m_e c^2} \right)^2 (1 + \cos^2 \theta) d\Omega \quad (4-10)$$

Thus in terms of the classical electron radius $r_e = e^2/m_e c^2$, the Thomson differential cross section is

$$\sigma_{\text{Th}}(\theta) = \frac{1}{2} r_e^2 (1 + \cos^2 \theta) \quad \text{cm}^2/\text{electron} \quad (4-11)$$

The structure of this differential scattering cross section per electron as a function of the scattering angle θ is shown in Fig. 4-2.

The total scattering cross section follows from integration over all scattering angles θ :

$$\sigma_{\text{Th}} = \int \sigma_{\text{Th}}(\theta) d\Omega = \int_0^\pi \frac{1}{2} r_e^2 (1 + \cos^2 \theta) 2\pi \sin \theta d\theta = \pi r_e^2 [-\cos \theta - \frac{1}{3} \cos^3 \theta]_0^\pi \quad (4-12)$$

i.e.,

$$\sigma_{\text{Th}} = \frac{8}{3} \pi r_e^2 \equiv \frac{8}{3} \pi \left(\frac{e^2}{m_e c^2} \right)^2 = 0.665 \text{ b} \quad (4-13)$$

It will be noted that the result is a function of r_e even though in the theory the electron has implicitly been treated as a point charge. On the basis of a naive geometrical interpretation of σ_{Th} one might consider $(8/3)^{1/2} r_e$ to represent an "effective" electron radius, but this must not be taken too literally.

The result is noteworthy in that it contains no energy-dependent term and predicts no change in wavelength upon re-emission of electromagnetic radiation. Since it stands for a cross section *per electron* it should, strictly, be written as ${}_e\sigma_{\text{Th}}$ and the corresponding *atomic* cross section as ${}_a\sigma_{\text{Th}}$ for which,

assuming there to be an independent interaction with each of the Z quasi-free electrons in the atom, we may write

$${}_a\sigma_{\text{Th}} = Z {}_e\sigma_{\text{Th}} = \frac{8}{3} \pi r_e^2 Z \quad (4-14)$$

This linear dependence upon Z provided the basis for the elucidation of atomic numbers of light elements by Barkla [Ba 11] and others. The cross section for scattering on particles heavier than electrons, e.g., on protons, is

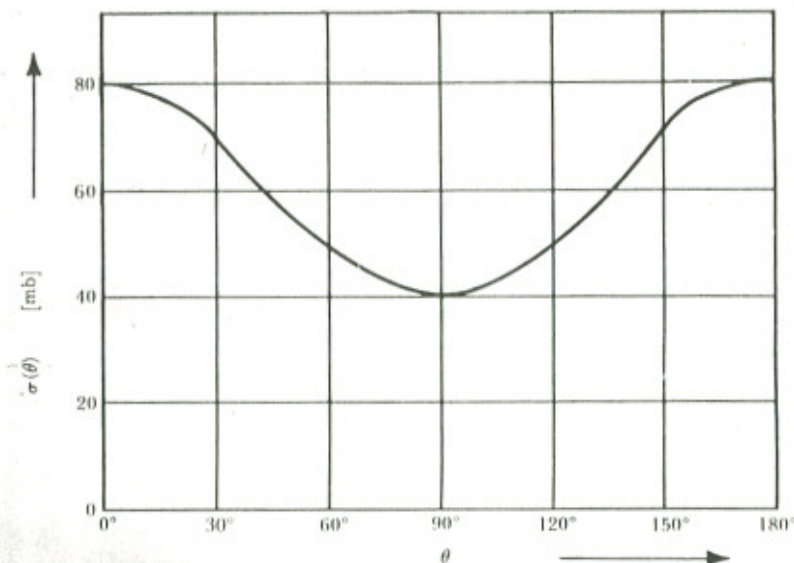


Fig. 4-2. Basic form of the differential cross section for Thomson scattering, as given by Eq. (4-11).

vanishingly small because of the inverse-square dependence upon the mass of the scattering body.

It is found that for γ -ray energies exceeding the electron binding energy but small in comparison with $m_e c^2 = 0.511 \text{ MeV}$, the cross section measured at small angles approaches Thomson's value, but when the scattering is observed at progressively larger angles there is a diminution in the intensity of coherently scattered radiation, offset by an increase in the incoherent portion whose wavelength is larger than that of the incident radiation.

4.2.2. COMPTON EFFECT

The effect in which there is a wavelength shift in incoherent scattering of electromagnetic radiation on quasi-free atomic electrons bears Compton's

name since he undertook the first experimental investigations [Co 22] and provided† a theoretical explanation [Co 23a, Co 23b, Co 24] which constituted early evidence for the corpuscular photon conception of electromagnetic radiation according to quantum ideas. The increase of wavelength as shown in Fig. 4-3, which corresponds to a decrease in energy upon scattering, can be derived from a consideration of relativistic momentum and energy conservation in a collision which is treated as though it were elastic (although

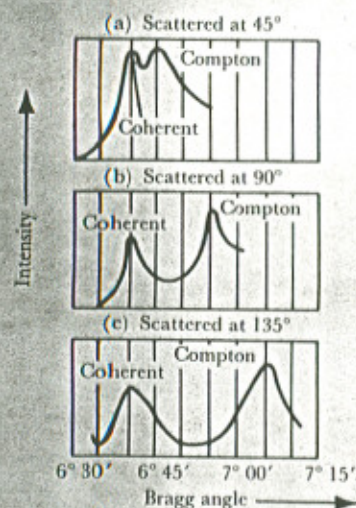


Fig. 4-3. Reproduction of Compton's measurements on x-ray lines (the $K\alpha$ lines from molybdenum) scattered from graphite, the left-hand peak in each case being the coherent line, of wavelength $\lambda = 0.71 \text{ \AA}$ and the right-hand peak the Compton line, displaced by an amount $\Delta\lambda$, which increases as $(1 - \cos \theta_\gamma)$ (from [Sm 65]). (Reprinted with permission of Pergamon Press Ltd.)

incoherent scattering on bound electrons constitutes an *inelastic* process). The Compton effect assumes importance when the γ energy becomes comparable with, or higher than, $m_e c^2 = 0.511 \text{ MeV}$. It is maximal around 1 MeV and is especially pronounced at fairly large scattering angles.

Figure 4-4 depicts the situation in which a photon of energy $h\nu$ and momentum $h\nu/c$ incident upon a stationary free electron is scattered through an angle θ_γ and emerges with an energy $h\nu'$ and momentum $h\nu'/c$. The electron recoils at an angle θ_e with an energy E_{kin} and momentum \mathbf{p} which may be sufficiently large to be treated relativistically. Conservation of momentum perpendicular to the scattering plane requires that all momentum vectors be coplanar. In the scattering plane, momentum conservation along the incident direction requires that

$$\frac{h\nu}{c} = \frac{h\nu'}{c} \cos \theta_\gamma + p \cos \theta_e \quad (4-15)$$

† Debye [De 23] independently gave a quantitative theoretical explanation. Bartlett [Ba 64b] gives a good description of the historical background.

and perpendicular thereto,

$$0 = \frac{h\nu'}{c} \sin \theta_\gamma - p \sin \theta_e \quad (4-16)$$

Energy conservation furnishes a third equation,

$$h\nu = h\nu' + E_{\text{kin}} \quad (4-17)$$

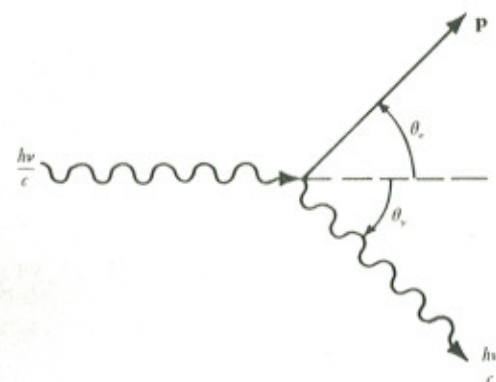


Fig. 4-4. Compton scattering of an incident photon (momentum $h\nu/c$) by a quasi-free electron through an angle θ_γ . The momentum of the scattered photon is $h\nu'/c$ ($< h\nu/c$); the electron recoils at an angle θ_e with a momentum \mathbf{p} .

which with the above and the relativistic energy-momentum relation [Eq. (1-10), Appendix A.2]

$$pc = [E_{\text{kin}}(E_{\text{kin}} + 2m_e c^2)]^{1/2} \quad (4-18)$$

can be manipulated to yield the following general results:

(a) For all incident photon energies the COMPTON SHIFT of wavelength is

$$\Delta\lambda \equiv \lambda' - \lambda \equiv \frac{c}{\nu'} - \frac{c}{\nu} = \lambda_C (1 - \cos \theta_\gamma) \quad (4-19)$$

and therefore increases with the scattering angle θ_γ . The maximum shift occurs when $\theta_\gamma = 180^\circ$ and takes the value $\Delta\lambda_{\text{max}} = 2\lambda_C$. The quantity

$$\lambda_C \equiv \frac{h}{m_e c} = 2.426 \, 21 \times 10^{-10} \text{ cm} \quad (4-20)$$

is termed the COMPTON WAVELENGTH of the electron and is numerically equal to the wavelength of a photon whose energy is $m_e c^2 = 0.511 \text{ MeV}$. Excellent

agreement has been obtained between measured and predicted Compton shifts.

(b) The outgoing photon energy in terms of the scattering angle is

$$\frac{E_{\gamma(\text{out})}}{E_{\gamma(\text{in})}} \equiv \frac{h\nu'}{h\nu} = \frac{1}{1 + \mathcal{E}(1 - \cos \theta_\gamma)} \quad (4-21)$$

where $\mathcal{E} \equiv h\nu/m_e c^2$ represents the "reduced" incident γ energy. When $\theta_\gamma = 0$ it follows that $\nu' = \nu$ for all incident energies \mathcal{E} , so that $\Delta\lambda = 0$ in the forward direction. The relation (4-21) represents an ellipse whose eccentricity increases with \mathcal{E} . For very low incident γ energies, when $\mathcal{E} \ll 1$, it reduces to a circle and indicates that $\nu' \approx \nu$ for all scattering angles θ_γ .

(c) The kinetic energy of the Compton recoil electron,

$$E_{\text{kin}} = h\nu - h\nu' \quad (4-22)$$

can be expressed in terms of θ_γ or θ_e as

$$E_{\text{kin}} = h\nu \frac{\mathcal{E}(1 - \cos \theta_\gamma)}{1 + \mathcal{E}(1 - \cos \theta_\gamma)} \quad (4-23)$$

$$E_{\text{kin}} = h\nu \frac{2\mathcal{E} \cos^2 \theta_e}{(1 + \mathcal{E})^2 - \mathcal{E}^2 \cos^2 \theta_e} \quad (4-24)$$

(d) The angles θ_γ and θ_e can be related to each other through the formula

$$\cot \theta_e = (1 + \mathcal{E}) \tan \frac{\theta_\gamma}{2} \quad (4-25)$$

which shows that the electron recoil angle θ_e cannot exceed 90 degrees.

(e) The maximum energy transfer to the electron, which occurs when the photon is back-scattered, namely when $\theta_\gamma = 180^\circ$ and $\theta_e = 0^\circ$, is

$$(E_{\text{kin}})_{\text{max}} = \frac{h\nu}{1 + \frac{1}{2\mathcal{E}}} \quad (4-26)$$

and in this case the Compton shift of wavelength is maximal.

4.2.3. COMPTON CROSS SECTION (KLEIN-NISHINA FORMULA)

The evaluation of the differential cross section is rather complicated, since it involves the use of relativistic wave mechanics (see Heitler [He 54, pp. 217 ff.] and Appendix F), and we therefore confine ourselves to citing results first derived by Klein and Nishina [Kl 29]. The differential collision cross section per electron in the case of a linearly polarized incident plane electromagnetic wave is, in the notation employed hitherto, and in terms of the angle Θ between the polarization directions of the incident and emergent quanta,

given by the KLEIN-NISHINA FORMULA:

$$\epsilon \sigma_{\text{C}}(\theta_\gamma)_{\text{pol}} \equiv \frac{d \epsilon \sigma_{\text{C}}}{d\Omega_\gamma} \bigg|_{\text{pol}} = \frac{1}{4} r_e^2 \left(\frac{\nu'}{\nu} \right)^2 \left(\frac{\nu}{\nu'} + \frac{\nu'}{\nu} + 4 \cos^2 \Theta - 2 \right) \text{ cm}^2 \text{ sr}^{-1}/\text{electron} \quad (4-27)$$

When the incident wave is *unpolarized*, the differential collision cross section per electron is obtained by calculating the mean value of the above expression averaged over all angles Θ , and this in terms of the scattering angle θ_γ yields the result

$$\begin{aligned} \epsilon \sigma_{\text{C}}(\theta_\gamma)_{\text{unpol}} &\equiv \frac{d \epsilon \sigma_{\text{C}}}{d\Omega_\gamma} \bigg|_{\text{unpol}} \\ &= \frac{1}{2} r_e^2 \left(\frac{\nu'}{\nu} \right)^2 \left(\frac{\nu}{\nu'} + \frac{\nu'}{\nu} - \sin^2 \theta_\gamma \right) \text{ cm}^2 \text{ sr}^{-1}/\text{electron} \end{aligned} \quad (4-28)$$

or, expressed in terms of \mathcal{E} on making use of the relationship (4-21),

$$\begin{aligned} \frac{d \epsilon \sigma_{\text{C}}}{d\Omega_\gamma} \bigg|_{\text{unpol}} &= \frac{1}{2} r_e^2 \{ [1 + \mathcal{E}(1 - \cos \theta_\gamma)]^{-3} [-\mathcal{E} \cos^3 \theta_\gamma \\ &\quad + (\mathcal{E}^2 + \mathcal{E} + 1)(1 + \cos^2 \theta_\gamma) - \mathcal{E}(2\mathcal{E} + 1) \cos \theta_\gamma] \} \\ &\quad \text{cm}^2 \text{ sr}^{-1}/\text{electron} \end{aligned} \quad (4-29)$$

In the case of low energies, \mathcal{E} is negligibly small, and this reduces to the Thomson differential cross section,

$$\frac{d \epsilon \sigma_{\text{C}}}{d\Omega_\gamma} \bigg|_{\text{unpol}} \xrightarrow{\mathcal{E} \rightarrow 0} \frac{d \epsilon \sigma_{\text{Th}}}{d\Omega_\gamma} = \frac{1}{2} r_e^2 (1 + \cos^2 \theta_\gamma) \text{ cm}^2 \text{ sr}^{-1}/\text{electron} \quad (4-30)$$

The expression (4-29) is depicted graphically in Fig. 4-5 in polar representation for various values of \mathcal{E} , and the angular distribution for various values of \mathcal{E} is shown in the usual representation in Fig. 4-6.

The TOTAL COLLISION CROSS SECTION is obtained by integration over all scattering angles,

$$\epsilon \sigma_{\text{C}} = \int \epsilon \sigma_{\text{C}}(\theta_\gamma) d\Omega_\gamma = \int_0^\pi \epsilon \sigma_{\text{C}}(\theta_\gamma) 2\pi \sin \theta_\gamma d\theta_\gamma \quad (4-31)$$

the end result being

$$\begin{aligned} \epsilon \sigma_{\text{C}} &= 2\pi r_e^2 \left\{ \frac{1 + \mathcal{E}}{\mathcal{E}^2} \left[\frac{2(1 + \mathcal{E})}{1 + 2\mathcal{E}} - \frac{1}{\mathcal{E}} \ln(1 + 2\mathcal{E}) \right] \right. \\ &\quad \left. + \frac{1}{2\mathcal{E}} \ln(1 + 2\mathcal{E}) - \frac{1 + 3\mathcal{E}}{(1 + 2\mathcal{E})^2} \right\} \text{ cm}^2/\text{electron} \end{aligned} \quad (4-32)$$

which, when ϵ is small, can to a good approximation be reduced [Le 47] to

$$\epsilon\sigma_C \cong \frac{8}{3}\pi r_e^2(1 - 2\epsilon + 5.2\epsilon^2 - 13.3\epsilon^3 + \dots) \quad \text{cm}^2/\text{electron} \quad (4-33)$$

In the limit $\epsilon \rightarrow 0$ this is equal to the Thomson value

$$\epsilon\sigma_C \xrightarrow{\epsilon \rightarrow 0} \epsilon\sigma_{Th} = \frac{8}{3}\pi r_e^2 \quad \text{cm}^2/\text{electron} \quad (4-34)$$

$\epsilon \sim 0$ (Thomson)

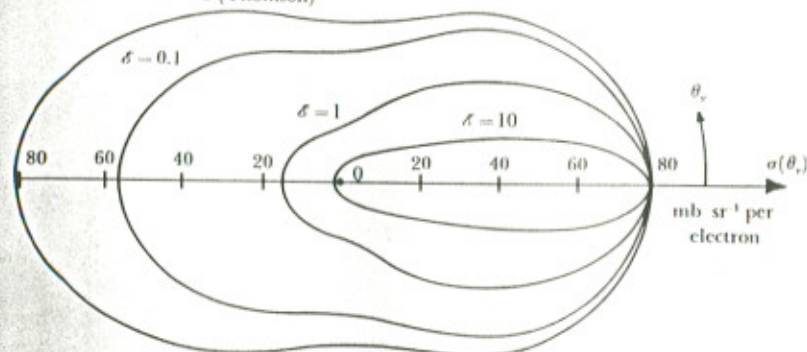


Fig. 4-5. Polar representation of the angular dependence of the differential cross section for Compton scattering of unpolarized radiation, as given by Eq. (4-29) for various values of the reduced incident energy $\epsilon \equiv h\nu/m_e c^2$ (adapted from [Da 52b]).

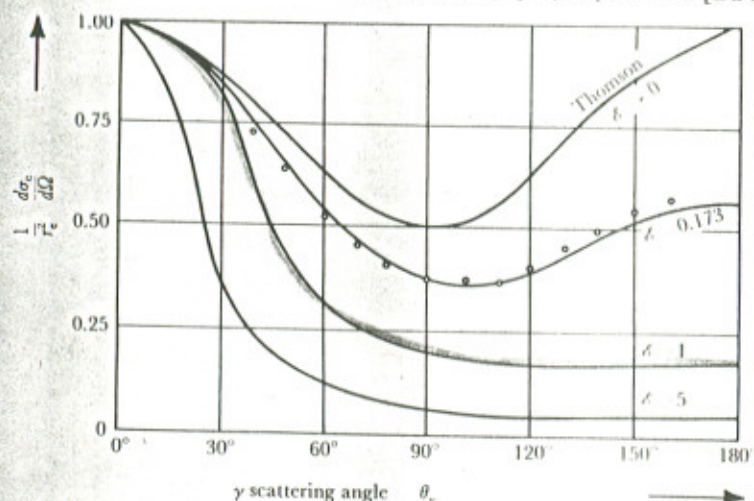


Fig. 4-6. Angular distribution of Compton-scattered γ quanta expressed as a normalized differential cross section $\sigma(\theta_\gamma)/r_e^2$ for various reduced incident energies $\epsilon \equiv h\nu/m_e c^2$. At $\epsilon = 0.173$ the curve is fitted to experimental data of Friedrich and Goldhaber [Fr 27] for scattering of 0.14-Å x rays in carbon (from [He 54]). (Used by permission of The Clarendon Press, Oxford.)

It is to be emphasized that the differential cross section (4-29) gives the number of photons scattered into unit solid angle at a mean scattering angle θ_γ , and that the total collision cross section (4-32) expresses the probability that a collision will occur in which a photon of energy $h\nu$ is removed from the collimated incident beam. It is therefore concerned with the energy taken out of the primary beam, and if the incident radiation is monochromatic, then this extracted energy is simply proportional to the number of Compton collisions. Not all of this energy is, however, scattered, since some of it is imparted to the electrons as recoil energy. The scattered energy is smaller than the incident energy by a factor $h\nu'/h\nu$, and in consequence the so-called ENERGY-SCATTERING CROSS SECTION σ_s which deals with the scattered γ energy, as against the extracted γ energy, is smaller than σ_C by this amount:

$$\sigma_s = \frac{h\nu'}{h\nu} \sigma_C \quad (4-35)$$

The transformation from the Klein-Nishina and derived formulae which feature the collision cross section per electron, $\epsilon\sigma_C$ to the corresponding expressions for $\epsilon\sigma_s$ is trivial therefore. A third concept which is sometimes encountered is the ENERGY-ABSORPTION CROSS SECTION σ_a which is simply the difference between the above two entities:

$$\sigma_a = \sigma_C - \sigma_s \quad (4-36)$$

and which represents the probability for the recoil kinetic energy

$$E_{kin} = h\nu - h\nu' \quad (4-37)$$

to be imparted to the electron in course of a Compton collision. It therefore concerns itself with the *transferred* energy which is subsequently dissipated within the target specimen through inelastic collisions and ionizing processes which the electron initiates.

Note that for clarity we have purposely referred to *energy-scattering* and *energy-absorption* cross sections, writing these as σ_s and σ_a respectively, in order to prevent confusion with the more usual *particle* scattering and absorption cross sections, σ_{sc} and σ_{abs} which we shall treat later.

The variation with γ energy of the various total cross sections defined above is indicated in Fig. 4-7 on a logarithmic energy scale.

One can also concern oneself with the differential and total cross sections for the Compton recoil electrons. No ambiguity exists in this case; the differential cross section can be derived from the photon collision cross section by multiplying the latter by an appropriate solid-angle factor:

$$\frac{d\epsilon\sigma}{d\Omega_e} = \frac{d\epsilon\sigma_C}{d\Omega_\gamma} \frac{d\Omega_\gamma}{d\Omega_e} = \frac{(1 + \epsilon)^2 (1 - \cos \theta_\gamma)^2}{\cos^3 \theta_e} \frac{d\epsilon\sigma_C}{d\Omega_\gamma} \quad (4-38)$$

and this is shown in polar representation in Fig. 4-8.

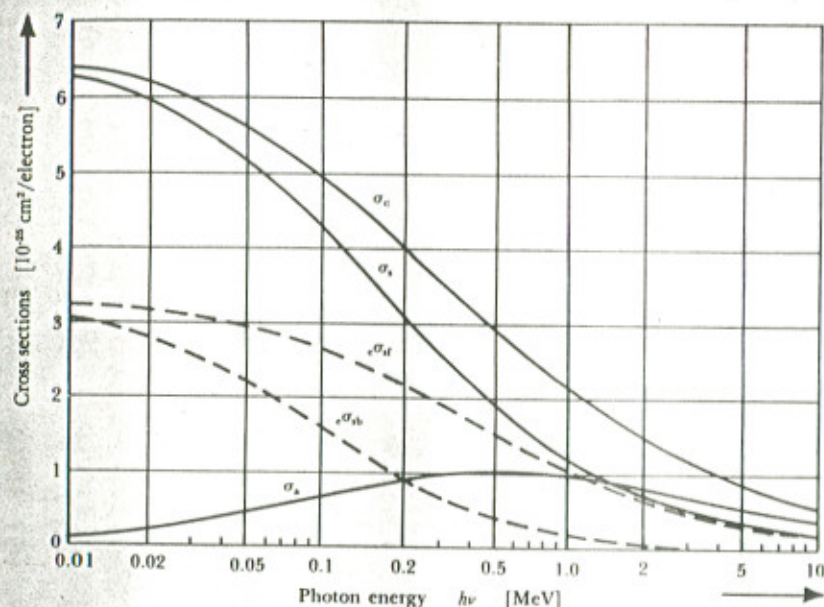


Fig. 4-7. Energy dependence of cross sections for the Compton effect. The full curves show the total collision cross section per electron σ_c together with its components σ_a , the absorption cross section and σ_s , the scattering cross section as given by (4-32), (4-35), and (4-36). Also depicted as dashed curves are the scattering cross sections per electron for the forward direction (σ_{st}) and the backward direction (σ_{sb}) (from [Da 65c]). (Used by permission of North-Holland Publishing Co.)

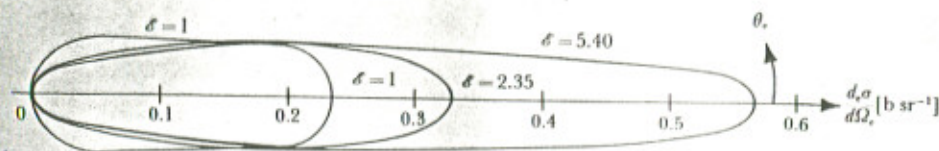


Fig. 4-8. Polar representation of the variation of the differential electron cross section for the Compton recoil electron emerging at an angle θ_e (from [Da 65c]).

4.2.4. ATOMIC COMPTON CROSS SECTION

Only at high incident photon energies is the binding energy of the electrons in an atom negligible and the linear formula

$${}_a\sigma = Z {}_e\sigma \quad (4-39)$$

applicable. At lower energies it is necessary to take account of the distributions

and momenta of the electrons in the atom, which involves a cognizance of the phase relations that exist.

The scattering is *coherent* when $h\nu = h\nu'$ and it is then appropriate to add up the individual *amplitudes*, rather than intensities, for each of the atomic electrons involved, whereas it is *incoherent* when $h\nu' < h\nu$ and one then sums the intensities. The atomic differential Compton cross section can accordingly

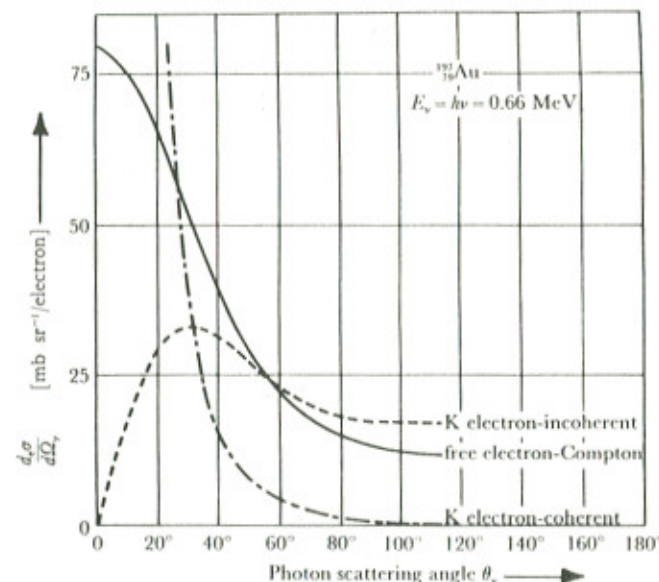


Fig. 4-9. Comparison of the angular distribution for the scattering of 0.66-MeV photons on gold, as calculated for Compton scattering on free electrons using the Klein-Nishina formula (4-28) for unpolarized radiation (solid curve), or for coherent scattering from electrons in the K shell [Br 57] (dot-dash curve) with the experimental results for *incoherent* K-electron scattering (dashed curve) (from [Mo 61]).

be represented as the sum of a coherent and an incoherent partial cross section:

$${}_a\sigma(\theta_\gamma) = {}_a\sigma_{\text{coh}}(\theta_\gamma) + {}_a\sigma_{\text{incoh}}(\theta_\gamma) \quad (4-40)$$

The calculation of the constituent terms is still in process of refinement. Figure 4-9 shows a comparison between the results furnished for the angular distribution of 0.66-MeV photons on gold by the Klein-Nishina formula and the calculated coherent differential cross section for scattering on bound electrons of the K shell, which shows more pronounced forward peaking. They may be contrasted with the measured incoherent cross section for K-shell electrons, whose angular dependence is of altogether different form.